# Confined Polymer Chains in a ϑ Solvent: A Model with Polymer−Solvent Interactions

**2 AUTHORS:**

Peter Cifra
Slovak Academy of Sciences
**96** PUBLICATIONS   **1,025** CITATIONS

Iwao Teraoka
Polytechnic Institute of New York University
**113** PUBLICATIONS   **2,884** CITATIONS

# Confined Polymer Chains in a Θ Solvent: A Model with Polymer−Solvent Interactions

**Peter Cifra\*,† and Iwao Teraoka\*,‡**

*Polymer Institute, Slovak Academy of Sciences, Dúbravská cesta 9, 842 36 Bratislava, Slovak Republic, and Herman F. Mark Polymer Research Institute, Polytechnic University, 333 Jay Street, Brooklyn, New York 11201*

ABSTRACT: Thermodynamics of polymer chains in the Θ condition confined to a space between two parallel walls was studied by using lattice Monte Carlo simulations. The Θ state was realized by allocating positive interaction to nearest-neighbor pairs of a polymer segment and a solvent molecule that is now explicitly included, rather than giving attractive interaction between polymer segments with no explicit solvent molecules present. The two models can be equivalent when used to specify the Θ state in unconfined solutions, but missing segment−solvent contacts at the wall make the two models different for confined solutions. The effectively attractive wall facilitates entry of polymer chains into narrow slits in the corrected model and lifts the segment density at sites adjacent to the walls. The dependence of the segment density near the wall on the distance from the wall follows a power law different from the one that holds for the conventional model of the Θ state. In particular, when the wall has explicit interaction with the polymer segments, our model makes the profile highly sensitive to the solvent quality. The corrected model explains enhanced adsorption in a poorer solvent reported in experiments.

## 1. Introduction

Computer simulations, both lattice and off-lattice systems, are widely being used to examine thermodynamic and other statistical properties of polymer in solution.[1] In most simulation systems, solvent molecules are not explicitly included. Each system has only one interaction parameter $\epsilon_{pp}$ that accounts for the interaction between nonbonded segment pairs in the polymer chains suspended in a vacuum. In athermal solutions, $\epsilon_{pp} = 0$. To represent a solution with a solvent worse to the polymer, $\epsilon_{pp}$ is turned negative. This practice has been employed broadly in the past to study the Θ state in lattice simulations[2−5] and in off-lattice simulations.[6,7] Theories for solutions in the Θ state have been using the same practice.[8−11]

Computer simulations and theoretical methods have been the primary tools to study the effect of geometrical confinement such as the one given by a slit and a channel on polymer solutions in various solvent conditions.[12−16] They include a Θ solvent and solvents that have a quality between athermal and Θ. As in unconfined solutions, the solution system in the confining geometries consists only of polymer chains. The solvent quality is adjusted by changing $\epsilon_{pp}$. The pore wall remains repulsive to the polymer throughout the change, thus precluding adsorption onto the walls of the confining geometries even in the Θ condition.

In real polymer solution systems, however, the change in the solvent quality is accomplished by adjusting the polymer−solvent interaction, not $\epsilon_{pp}$. The change is made possible through a change in the temperature or the mixing ratio of a good solvent and a poor solvent or a nonsolvent. When the polymer solution is in contact with a porous medium, poorer solvents promote adsorption of the polymer onto the pore walls. It is well-known in size exclusion chromatography that the mobile phase

needs to be sufficiently good to the analyte polymer. Otherwise, the injected polymer may be retained by the stationary phase, indicating adsorption of polymer onto the pore wall.[17]

Obviously, the shortcoming of the existing theories and simulation methods arises from transplanting the convention employed in the bulk systems into the confined systems. In the present report, we explicitly include solvent molecules by regarding the unoccupied sites as being occupied by solvent molecules in lattice Monte Carlo simulations for confined polymer solutions. We change the solvent−polymer interaction, not the polymer−polymer interaction, to bring the solution to the Θ condition. Incidentally, the wall becomes attractive to the polymer since the segments prefer the walls to the solvent. We demonstrate that the partitioning and other statistical properties of the confined polymer chains are greatly different in this modified Θ condition from those in the conventional Θ condition. The same precaution will be needed whenever simulations and theories deal with polymer solutions that are in contact with any third components.

## 2. Lattice Model for Confined Chains in a Θ Solvent

In many models for polymer solutions in discrete and continuous spaces, polymer chains are suspended in a vacuum; solvent molecules are not explicitly included in the system.[2−15] As a result, interactions other than chain connectivity are present only between a nonbonded pair of polymer segments (P−P contact). In lattice chain models, for instance, there is a well-defined interaction $\epsilon_{pp}$ between nearest-neighbor nonbonded pair of segments, as indicated by dashed lines in part a of Figure 1, where the solid line represents the chain. We call this model a PP model.

To realize the Θ condition in the PP model, net repulsion between polymer segments due to the excluded volume is compensated by attractive interaction.

† Slovak Academy of Sciences.
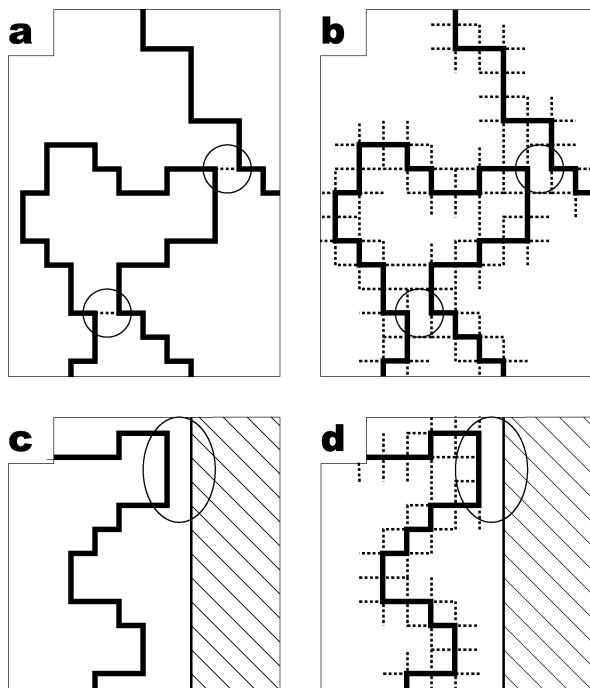‡ Polytechnic University.
* Corresponding author.

**Figure 1.** Models for interacting polymer chains in solution on a two-dimensional version of a cubic lattice. Parts a and b illustrate the PP model and the SP model, respectively, for bulk solutions. Parts c and d explain the two models for solutions in contact with a wall.

In the cubic lattice Monte Carlo simulations, it was found that $\epsilon_{pp}/k_B T = -0.2693$, where $k_B T$ is the thermal energy, gives the necessary attraction.[18] Decreasing the single parameter $\epsilon_{pp}$ from zero represents polymer solutions in solvents with qualities between the athermal solvent and the Θ solvent or worse than the Θ solvent. In real systems, however, $\epsilon_{pp}$ is specified once the polymer is given.

We propose an alternative to the PP model to describe polymer chains in the Θ solvents. Our model explicitly contains solvent molecules and considers the interaction between the polymer segment and the solvent molecule. In the lattice model, each empty site is filled with a solvent molecule. Now the system has two more parameters $\epsilon_{sp}$ and $\epsilon_{ss}$ that account for the interaction for a polymer–solvent pair (P–S contact) and the interaction for a solvent–solvent pair (S–S contact), respectively. The S–P contacts are indicated by dashed lines in Figure 1b. Since the absolute level of the energy is arbitrary, we can set $\epsilon_{ss} = 0$. For simplicity, we additionally set $\epsilon_{pp} = 0$. The model, which we call an SP model, regulates the solvent quality only through $\epsilon_{sp}$. The rationale is that real polymer solutions are brought to the Θ condition or another solvent condition by changing the interaction of the polymer with the solvent. In the SP model, increasing $\epsilon_{sp}$ from zero corresponds to degrading the solvent quality from good to Θ and beyond.

In lattice chain models, in general, the state of the system depends on the interactions only through the Flory parameter $\chi$ defined as $\chi = Z[\epsilon_{sp} - (\epsilon_{pp} + \epsilon_{ss})/2]/k_B T$, where $Z$ is the lattice coordination number. Therefore, the PP model and the SP model should behave identically if

$$[\epsilon_{sp} \text{ of the SP model}] = -\tfrac{1}{2}[\epsilon_{pp} \text{ of the PP model}] \quad (1)$$

When applied to the Θ condition, $2\epsilon_{sp}/k_B T = 0.2693$ should give the necessary interaction to the SP model. Both models have $\chi = 0.2693 \times 3$ in the cubic lattice.

The equivalency of the two models through eq 1 holds only for systems consisting of polymer chains and solvent molecules such as bulk solutions. The situation will be greatly different when a third component such as a wall is present. In the PP model in contact with an impenetrable wall (hatched region in Figure 1c), placing a part of the chain in the layer nearest to the wall does not change the energy unless the interaction for a polymer–wall contact is explicitly introduced. The energy does change in the SP model because of loss of polymer–solvent contacts (Figure 1d).

Let us consider an SP model for a polymer solution in contact with a wall. Now the system has two more interactions, $\epsilon_{pw}$ for a polymer–wall contact and $\epsilon_{sw}$ for a solvent–wall contact. We set $\epsilon_{sw} = 0$ for simplicity. Moving a polymer chain can change its energy in two ways: (1) Formation of a P–P contact changes the energy by $-2\epsilon_{sp}$; when a solvent molecule comes in to remove such a contact, the change is $2\epsilon_{sp}$. (2) Movement of a polymer segment into a solvent-filled site in the layer nearest to the wall from a site in the next-nearest layer changes the energy by $\epsilon_{pw} - \epsilon_{sp}$, since the chain adds a contact with wall and loses a contact with solvent. The reverse motion changes the energy by $-(\epsilon_{pw} - \epsilon_{sp})$. In Figure 1d, the chain has extra energy of $(\epsilon_{pw} - \epsilon_{sp}) \times 3$ compared with a chain of the same configuration surrounded by solvent molecules.

The polymer–wall interaction can be introduced in the PP model as well. Since solvent molecules are absent, $\epsilon_{sw} = 0$. Nonzero $\epsilon_{pw}$ has been used in many simulation studies on adsorption.[19–25]

As in the Flory parameter, we can define a polymer–wall effective interaction parameter $\chi_{pw}$ for adsorption as

$$\chi_{pw} = [(\epsilon_{pw} + \epsilon_{ss}) - (\epsilon_{sp} + \epsilon_{sw})]/k_B T \quad (2)$$

to account for the energy change when a polymer segment displaces a solvent molecule on a site in the layer next to the wall by moving from a site in the second layer. In the PP model, $\chi_{pw} = \epsilon_{pw}/k_B T$, and in the SP model, $\chi_{pw} = (\epsilon_{pw} - \epsilon_{sp})/k_B T$. If the wall is neutral to the polymer, i.e., $\epsilon_{pw} = 0$, then $\chi_{pw} = 0$ in the PP model and $\chi_{pw} = -\epsilon_{sp}/k_B T$ in the SP model. Thus, in the SP model, polymer segments prefer to sit on sites next to the wall when $\epsilon_{sp} > 0$ as in the Θ solvent. The positive segment–solvent interaction leads to an effective adsorption of polymer, in agreement with experimental facts.[17] The two models can have the same $\chi_{pw}$ by designating different values of $\epsilon_{pw}$. It is obvious, however, that the SP model with $2\epsilon_{sp}/k_B T = 0.2693$ will let the system behave as in real Θ systems without introducing artificial $\epsilon_{pw}$.

In the system of a given polymer and a wall, use of a different solvent changes $\epsilon_{sp}$ and $\epsilon_{sw}$ simultaneously. For the theories and simulations to describe such a system, it is necessary to introduce a nonzero $\epsilon_{sw}$, although we assumed $\epsilon_{sw} = 0$ in our SP model. As we have noted, what matters is $\chi_{pw}$. Alternatively, the condition of $\chi_{pw} = -\epsilon_{sp}/k_B T$ may be realized in experiments by chemically modifying the pore wall to have $\epsilon_{pw} = \epsilon_{sw}$ for each solvent used ($\epsilon_{ss} = 0$). Methods to attach various moieties to the surface of porous silica, for instance, are well-known.[28]
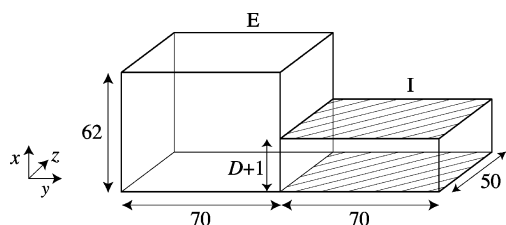
**Figure 2.** Simulation box for partitioning studies. Box I has a pair of impenetrable walls.

## 3. Methodology

We performed two types of simulations on a cubic lattice: (1) simulation of an ensemble consisting of an unconfined space and a slitlike pore for direct equilibrium of chains between the two spaces and (2) simulation of a canonical ensemble of chains in the slit space. The two types are explained separately below.

(1) This type of simulation was described previously.[13,14] Two boxes, box E representing the exterior (bulk) phase and box I representing the interior slit pore, are connected to each other (Figure 2). The box E has dimensions of $62 \times 70 \times 50$ (the unit length is a lattice unit) along the $x$, $y$, and $z$ directions, respectively. In box I of $(D + 1) \times 70 \times 50$, there are two solid walls at $x = 0$ and $D$ to form a slit space. In the $x$ and $z$ directions, periodic boundary conditions apply to all pairs of opposite walls of the boxes except the solid walls. In the $y$ direction, a combined period of $70 + 70$ repeats itself. As a result, both mouths of box I are connected to box E. The polymer beads are not allowed to occupy the sites on the solid walls.

Chains consisting of $N = 100$, 200, and 500 segments were generated as self-avoiding walks on the cubic lattice and equilibrated using reptation moves and the Metropolis algorithm.[29] In reptation (slithering-like motion), we need to evaluate a change of interactions, $E_{new} - E_{old}$, at the new "head" and the old "tail" segment positions only. The Boltzmann factor with the resulting energy change, $\exp(-(E_{new} - E_{old})/k_B T)$, is then compared to a random number in the range of (0, 1). The trial move is accepted as a new configuration if the factor is greater than the random number.[13,14] Simulation starts usually from an initial random configuration not far from the required thermodynamic state. In the simulation, chains are free to move by reptation between the two boxes. Therefore, the simulation provides equilibrium concentrations of the chains in the two boxes.[26,27] There is no need to calculate the confinement free energy from the chemical potentials of the chains in the two boxes. The overall ensemble is canonical and features the aspects known as the Gibbs ensemble because it is ensured that the two chemical potentials are equal. The volume fractions $\phi_I$ and $\phi_E$ of the chains in boxes I and E fluctuate during equilibration without changing the total number of chains in the system. The ratio $\phi_I/\phi_E$ of the average volume fractions gives the partition coefficient $K$. The volume fractions $\phi_E$ (denoted henceforth also as $\phi$ where appropriate) up to 0.7 were used for $\Theta$ chains.

(2) Simulation of chains in the slit space only was used to obtain details of segment density profiles of long chains including those adsorbed onto the walls under explicit $\epsilon_{pw} < 0$. The slit space has dimensions of $(D + 1) \times 100 \times 100$, with two walls present at $x = 0$ and $D$. A single slit width $D = 50$ was used. In the other two directions, periodic boundary conditions were enforced.

**Table 1. $\Theta$ and Athermal Chains Used in Simulations**

| | $\Theta$ | | athermal | |
| --- | --- | --- | --- | --- |
| $N$ | $R_{g0}$ | $\phi^*$ | $R_{g0}$ | $\phi^*$ |
| 100 | 5.34 | 0.207 | 6.46 | 0.120 |
| 200 | 7.66 | 0.145 | 9.74 | 0.0720 |
| 500 | 12.26 | 0.0913 | 16.81 | 0.0359 |
| 1000 | 17.52 | 0.0635 | 25.52 | 0.0208 |

Chains with $N = 500$ and 1000 were simulated in the canonical ensemble on a cubic lattice in the slit. The density profile $\phi(x)$ is defined as the mean fraction of the sites occupied by polymer segments in the layer at distance $x$ from one of the walls. We display a symmetrized profile, $[\phi(x) + \phi(D - x)]/2$, in the present report.

For the second type of simulation, we used combination of reptation moves and the configurational bias Monte Carlo (CBMC) moves with chain regrowth along favorable configuration energy. A reptation Monte Carlo step is defined as series of $N$ reptation moves. Each reptation Monte Carlo step is followed by a CBMC move. The latter move is realized by discarding a head portion of the chain (10−200 segments) and regrowing the same number of segments. In reptation, we used persistent reptation, in which the head and tail of a given chain are interchanged only after an unsuccessful move. In the CBMC move, this interchange occurs after each regrowth. The combined moves, which were employed earlier,[25] facilitate exploring different configurations by systems that are otherwise extremely slow to do so, especially by systems containing adsorbed long chains. Details on CBMC method can be found elsewhere.[1]

It is common to both types of simulation that switching from the PP model to the SP model does not require a change of simulation algorithm or lead to an increase of computing time. We have only to calculate the change in the number of contacts between polymer segments and the empty sites in place of the number of contacts between segments. Fortunately, these contacts are already enumerated in the PP model in every Monte Carlo move (whether reptation, kink jump, or another type) to evaluate the interaction energy.

Keeping track with the number of contacts during simulation is easy. Two simple rules apply: (1) Formation of a P−P contact pair changes the energy by $-2\epsilon_{sp}$, since it accompanies annihilation of two S−P contacts. In reverse, breakage of a P−P contact changes the energy by $2\epsilon_{sp}$. (2) When a polymer segment enters the layer nearest to the wall, the chain loses $\epsilon_{sp}$. It may gain the interaction with the wall, $\epsilon_{pw}$, for an interacting wall. Leaving this layer leads to the opposite changes.

The root-mean-square radii of gyration $R_{g0}$ of chains used in the present study in unconfined dilute solution are listed in Table 1 for $\Theta$ chains and athermal chains. Also listed are the overlap volume fraction $\phi^*$ defined as $\phi^*[2^{1/2}(R_{g0} + \alpha)]^3 = N$, where $\alpha$ represents the thickness of a coating to account for the finite size of each lattice site.[30] The values of $\alpha$ is 0.199 for athermal chains and 0.204 for $\Theta$ chains.[13] We verified in unconfined space that $R_{g0}$ is identical in the SP model and the PP model in the $\Theta$ condition.

## 4. Results and Discussion

**A. Overview.** We first take a quick look at the difference of properties between the PP model and the SP model. Figure 3 shows the segment density profile $\phi(x)$ obtained by using the two models for chains of $N =$
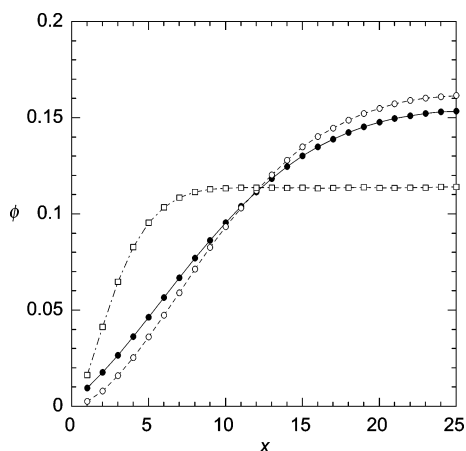
**Figure 3.** Segment density profile $\phi(x)$ across a slit of width $D = 50$, obtained using the SP model (closed circles) and the PP model (open circles) for Θ chains of $N = 1000$. Only a left half of the profile is shown as a function of the distance $x$ from the wall. The profile for athermal chains is also shown (open squares).

1000 confined to a slit of $D = 50$. The profile for athermal chains of the same length in the same slit width is shown for reference. The average segment density $\phi_{av}$ in the slit is 0.1020 for the three systems. Only a half of the symmetrized profile is shown. The athermal solution in the slit is already in the semidilute region ($\phi_{av}/\phi^* = 4.9$). Strong repulsive interactions between segments due to excluded volume push them toward the walls.[27,31-34] Therefore, the density profile has a broad plateau in the middle of the slit, and the depletion layer has a thickness equal to the correlation length in the semidilute solution which is shorter than $R_{g0}$.

In contrast, the profiles in the Θ solvent do not have a plateau because three-body interactions are still weak at this concentration ($\phi_{av}/\phi^* = 1.6$). The most striking difference between the two Θ profiles is seen near the wall. The density at sites near the wall is higher in the SP model than it is in the PP model. As opposed to a decline of $\phi(x)$ to zero along a parabola on approaching the wall in the PP model, the profile of the SP model approaches zero almost linearly with decreasing $x$. The higher density near the wall in the SP model is ascribed to $\chi_{pw} < 0$. We will discuss the difference in more detail later. It may appear that $\phi(x)$ of the athermal chains exhibits a linear approach to zero at the wall, but it is caused by the small number of lattice points at $x <$ correlation length which is estimated as ca. 4.

Figure 4 compares the partition coefficient $K$ as a function of $\phi_E$, the average segment density exterior to the slit, obtained by using the two models. Chains of $N = 100$ were equilibrated with a slit of $D = 12$. Obviously, the negative $\chi_{pw}$ raises $K$, especially at low $\phi_E$. In the dilute solution limit, the increase in $K$ is nearly 100%. It is common to the two models that $K$ is nearly flat at low concentrations because the second virial coefficient is zero in the Θ condition. The increase in $K$ (stronger penetration) occurs at around the same concentration. For athermal chains, in contrast, the plot of $K$ has a positive slope at $\phi_E = 0$. Polymer chains are driven into the pore at a higher proportion by the binary interaction that is stronger in the unconfined space where concentration is higher.[35]

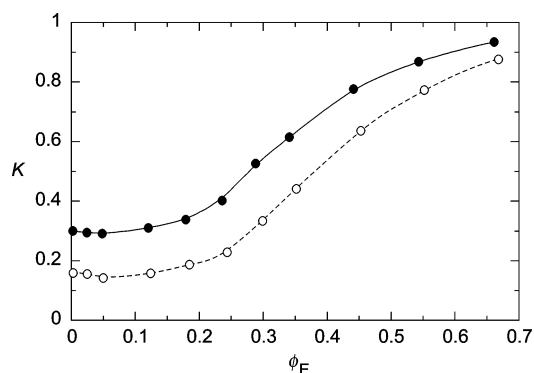**B. Partitioning at Low Concentrations.** Now we examine the difference between the two models in more



**Figure 4.** Partition coefficient $K$ of Θ chains ($N = 100$) with a slit of width $D = 12$ obtained using the SP model (closed circles) and the PP model (open circles), plotted as a function of the volume fraction $\phi_E$ in the unconfined space. The lines are for guides for the eye.
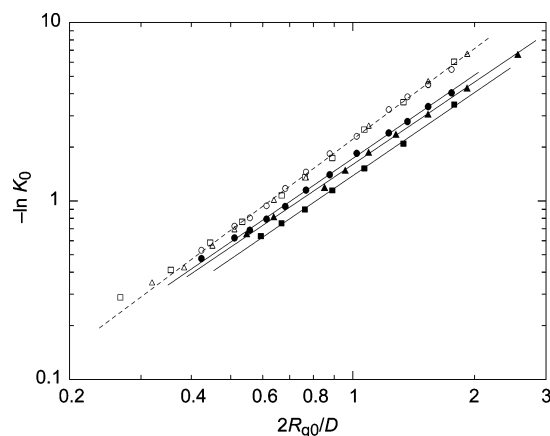


**Figure 5.** Free energy increase, $-\ln K_0$, of a Θ chain due to confinement by a slit, plotted as a function of the chain-to-slit size ratio, $2R_{g0}/D$. The results of the PP model for $N = 100$, 200, and 500 are shown as open squares, triangles, and circles, respectively. Those of the SP model for $N = 100$, 200, and 500 as closed squares, triangles, and circles, respectively. The dashed and solid lines are the optimal fits by a power law for data at $2R_{g0}/D > 0.7$ for all chain lengths of the PP model and each chain length in the SP model.

detail. Figure 5 examines the partition coefficient $K_0$ in the dilute solution limit obtained for three chain lengths with slits of various widths. The coefficients were obtained at sufficiently low concentrations, $\phi_E < 0.0025$. The figure shows $-\ln K_0 > 0$ (free energy penalty on a chain entering the slit) as a function of the chain dimension $2R_{g0}$ of a single chain in the unconfined solution relative to $D$. The results of the PP model for $N = 100$ and 200 were obtained earlier.[13]

We note that $K_0$ is determined by $2R_{g0}/D$ within the PP model. At $2R_{g0}/D > 0.7$, the data obtained for different chain lengths fall on a straight line with a slope of 1.69. This exponent is less than the one predicted in the scaling theory (=2).[36] The difference is still controversial.[13] The exponent is almost identical to the one for athermal chains.[13,27,30]

The data for the SP model are located lower than those for the PP model at the same $R_{g0}/D$. The effective attractive interaction with the wall ($\chi_{pw} < 0$) makes the entrance of Θ chains easier. For a given chain length, $-\ln K_0$ appears to follow a power relationship with $2R_{g0}/D$, at least in the range of $2R_{g0}/D > 0.7$. The exponent is between 1.54 and 1.56 for the three chain lengths, smaller compared with the exponent for the PP model. Unlike the results for the PP model, the data for
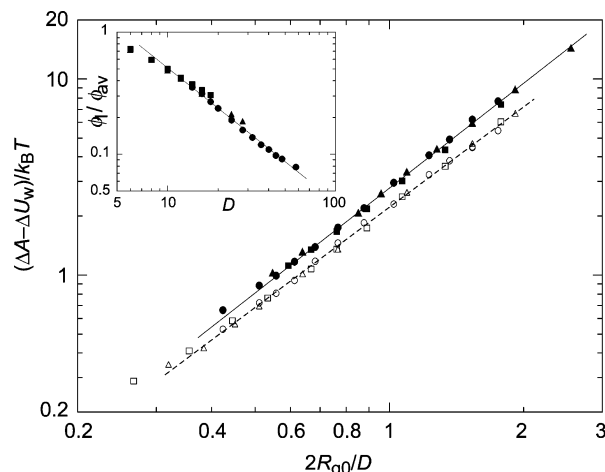
**Figure 6.** Free energy increase minus the change in the interaction with the walls, $\Delta A - \Delta U_w$, is plotted as a function of $2R_{g0}/D$. The symbols are identical to those in Figure 4. The dashed and solid lines are the optimal fits by a power law for data at $2R_{g0}/D > 0.7$ for the PP model and the SP model, respectively. The inset shows the ratio of the segment density in the first layer to the average density in the slit as a function of $D$ for the three chain lengths of the SP model.



**Figure 7.** Partition coefficient $K_0$ of a polymer chain of $N = 500$ in the SP and PP models with a slit of $D = 24$, plotted as a function of Flory's interaction parameter $\chi$ divided by lattice coordination number $Z$. The lines connecting the closed circles (SP model) and the open circles (PP model) are for eye guide. The inset shows $(\Delta A - \Delta U_w)/k_B T$ for the two models.

different chain lengths do not lie on a master curve. It is easier for shorter chains to enter the slit than longer chains at the same $R_{g0}/D$, or the effective adsorption is stronger for shorter chains.

To find how much the negative $\chi_{pw}$ facilitates the partitioning of SP chains, we define the energy difference $\Delta U_w$ due to the absence of solvent molecules on the sites occupied by the walls, i.e., missing S–P contacts. Suppose there is a single chain in the slit formed by a pair of walls of $L \times L$ separated by $D$. Then, $\Delta U_w = -2\epsilon_{ps}\phi_1 L^2$, where $\phi_1 = \phi(1)$ is the density in the first layer. Since $N = \phi_{av}L^2(D - 1)$

$$\Delta U_w = -2\epsilon_{ps}(\phi_1/\phi_{av})N/(D - 1) \tag{3}$$

At sufficiently low concentrations in the slit, $\phi_1/\phi_{av}$ is independent of the concentration. Therefore, eq 3 is valid as long as $\phi_{av} \ll \phi^*$. The ratios were calculated in our simulations for the SP model.

In the PP model, $\Delta U_w = 0$. Note that, in both models, the confinement changes the number of P–P contacts. (In the SP model, one P–P contact is equivalent to the absence of two S–P contacts.) Therefore, $\Delta U_w$ does not account for all of the energy change upon confinement. The energy change occurs also in the PP model. For athermal chains, in contrast, the confinement changes the entropy only.

The partition coefficient $K_0$ is related to the free energy change $\Delta A$ upon confinement through

$$-\ln K_0 = \Delta A/k_B T \tag{4}$$

We divide $\Delta A$ into the energy change $\Delta U$ that includes $\Delta U_w$ and the entropy change times temperature, $T\Delta S$. Then, $\Delta A - \Delta U_w = (\Delta U - \Delta U_w) - T\Delta S$. Figure 6 shows a plot of $(\Delta A - \Delta U_w)/k_B T$ as a function of $2R_{g0}/D$. Unlike in Figure 5, the data for the SP chains of different lengths are on a common straight line with a slope of 1.78. The latter indicates that $T\Delta S$ dominates $\Delta A - \Delta U_w$ since the decrease in the conformational entropy depends on the chain length and the slit width through $R_{g0}/D$, but the other term, $\Delta U - \Delta U_w$, does not. In fact, $\Delta U - \Delta U_w$, which is the energy change due to the
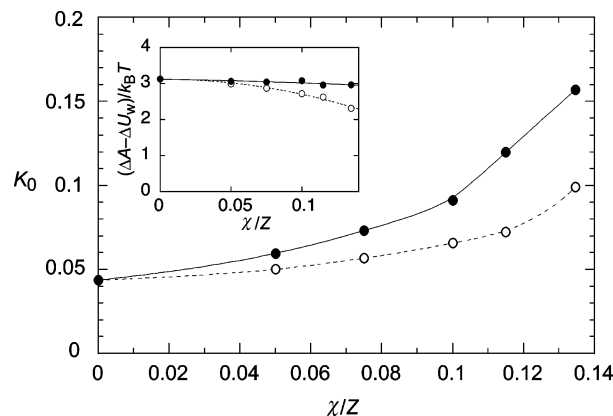
change in the number of P–P contacts, should be proportional to $N/D$. The proportionality is explained as follows: Most of the P–P contacts occur within a partial chain of $g$ segments that spans across the slit. In the $\Theta$ condition, $g^{1/2} \cong D$. The number of the contacts within the partial chain is $\sim g^2/D^3 \cong D$. For the whole chain, the number is $\sim (N/g)D \cong N/D$.

In Figure 6, the data for the SP model are located above the data for the PP chains that are identical to $-\ln K_0$ in Figure 5. The SP chains experience a greater decrease in the entropy when confined than the PP chains do. Obviously, the negative $\Delta U_w$ enables the chains to endure a greater $-\Delta S$. The difference, together with the inset of Figure 6, will be discussed in part C of this section.

The PP model and the SP model can be used for any solvent quality between athermal and $\Theta$ by varying $\epsilon_{PP}$ and $\epsilon_{SP}$, respectively. Two-box simulations were conducted for chains of $N = 500$ with a slit of $D = 24$ for pairs of $\epsilon_{PP}$ and $\epsilon_{SP}$ that satisfy eq 1, i.e., for the same $\chi$. The volume fraction of the chains was sufficiently low in the exterior solution, and therefore the partition coefficients obtained represent their dilute-solution limits $K_0$. The result of $K_0$ is shown in Figure 7 as a function of $\chi/Z$. The two models are identical in the athermal solution ($\chi = 0$). As the solvent turns poorer, $K_0$ increases for both models, but the increase is greater for the SP model. The increase for the PP model is mostly due to contraction of the chains.

In the SP model, the more negative $\chi_{pw}$ upon increasing $\epsilon_{sp}$ promotes polymer–wall contacts, resulting in a greater $K_0$ compared with that of the PP model. As we did in Figure 6, we estimate the direct wall interaction $\Delta U_w$ using the density profile data. The inset shows a plot of $(\Delta A - \Delta U_w)/k_B T$ as a function of $\chi/Z$. In contrast to a decrease for the PP model, the SP model exhibits nearly a constant $\Delta A - \Delta U_w$. For the range of $\chi/Z$ studied, $-\Delta S$ did not change appreciably for the SP chain. We consider that the decrease in $-\Delta S$ by the chain contraction with an increasing $\chi$ was counterbalanced by the increase that has resulted from the greater perseverance an SP chain endures because of the attractive $\chi_{pw}$ and the concomitant increase in the segment density near the walls.

It is instructive to see how the polymer–wall interaction alone changes a system that is free of any other
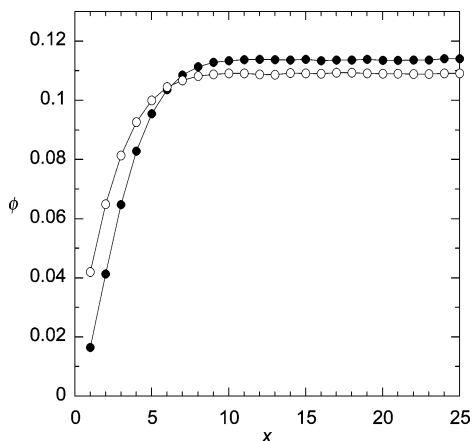
**Figure 8.** Density profiles of athermal chains of $N = 1000$ in a slit of width $D = 50$ in the absence (closed circles) and presence (open circles) of the interaction $\epsilon_{pw}$ between the wall and a polymer segment. When present, $\epsilon_{pw}/k_B T = -0.13465$ was used to give the same $\chi_{pw}$ as the one for the Θ state of the SP model.
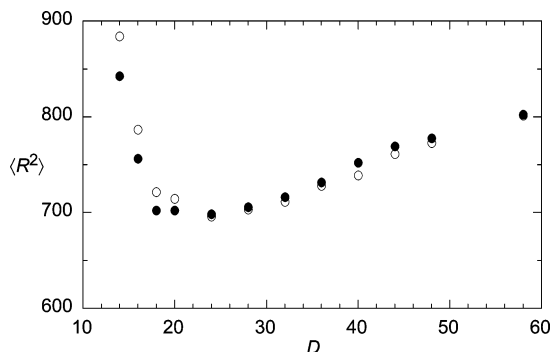


**Figure 9.** Mean-square end-to-end distance $\langle R^2 \rangle$ of Θ chains of $N = 500$ confined to slits of various widths $D$ from partitioning studies. Closed circles are for the SP model, and the open circles are for the PP model.

interactions. To provide the athermal chains with the same $\chi_{pw}$ as the one for the SP model in the Θ condition, we conducted a slit-only simulation for athermal chains by adding $\epsilon_{pw} = -0.2693/2$. The segment density profile is compared in Figure 8 for athermal chains of $\epsilon_{pw} = 0$ and $-0.2693/2$. The average volume fraction is $\phi_{av} = 0.1020$ in the two systems. The negative $\chi_{pw}$ has increased the segment density at sites near the walls, as it did in the SP model. Obviously, the SP model in the Θ condition provides the polymer chains with a considerable attraction to the wall.

The difference between the SP model and the PP model is also manifested in the mean square end-to-end distance $\langle R^2 \rangle$ of polymer chains in the slit. Figure 9 compares $\langle R^2 \rangle$ at different slit widths in the two models. It is common that $\langle R^2 \rangle$ first decreases with decreasing $D$ before it starts to rise. This behavior was ascribed earlier to lateral squeezing of chains with decreasing $D$, followed by elongation in the direction parallel to the walls.[37] There is a small difference in the two models. When $D/2 > R_{g0} (\cong 12.26)$, the two $\langle R^2 \rangle$ are nearly identical. When $D/2 < R_{g0}$, $\langle R^2 \rangle$ of the PP model rises more quickly with decreasing $D$. We consider that a lack of effective adsorption with the walls in the PP model forces the chains to stay away from the walls and to adopt a more extended conformation along the slit walls. In other words, the PP model represents more narrow slits for the same $D$. Note that the unconfined chain has $\langle R^2 \rangle = 901.8$. In the range of $D$ used in partitioning
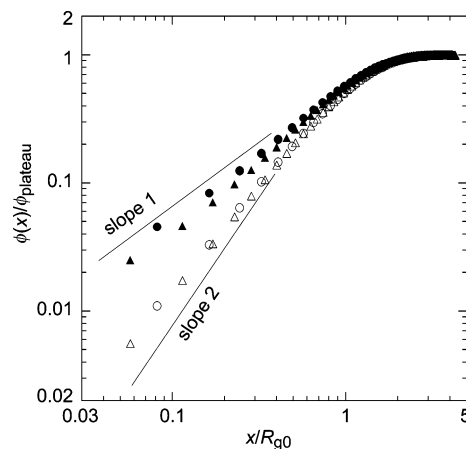


**Figure 10.** Segment density profile $\phi(x)$ of weakly confined Θ chains at low concentrations, normalized by the respective peak value at the plateau, $\phi_{plateau}$, is plotted as a function of the distance $x$ from the wall divided by $R_{g0}$ of the chain. The chain lengths are $N = 500$ (circles) and 1000 (triangles). Closed and open symbols represent the SP and PP models, respectively.

studies, the confinement is still not sufficiently strong to elongate the chain in the unrestricted directions of the slit. The situation is similar in athermal chains. Confinement as strong as $2R_{g0}/D > 2.5$ is needed for their $\langle R^2 \rangle$ to exceed the one in unconfined solution.[30]

**C. Density Profiles.** The segment density profiles of Θ chains in a broad slit are compared in Figure 10. It shows $\phi(x)/\phi_{plateau}$, the density normalized by its plateau value, as a function of $x/R_{g0}$ for the SP and PP models of $N = 500$ and 1000 in the Θ condition. Only a half of the symmetrized profile is shown. The slit widths are $D = 100$ for $N = 500$ ($2R_{g0}/D \cong 0.25$) and $D = 150$ for $N = 1000$ ($2R_{g0}/D \cong 0.23$). Since $R_{g0}$ is the only length scale in the system, the normalized density should be a function of $x/R_{g0}$.[31,32]

The two profiles of the PP model almost lie nearly on top of each other. Toward the walls, the data are on a power law of $\phi(x)/\phi_{plateau} \sim (x/R_{g0})^{1.66}$. The exponent in the power law is less than two, the theoretically predicted exponent.[32] In contrast, the two profiles of the SP model are not on a common curve, as the free energy data were not in Figure 5. Furthermore, the two profiles exhibit an upward deviation from a power law with approaching the walls. When 0.3 is added to $x$, the two sets of data for the PP model are on a common straight line with a slope close to 2 (not shown). It was shown earlier[33,34,38,39] that adding a positive penetration depth (extrapolation length[31]) $\gamma$ to $x$ improves the overlapping of the plots ($\phi(x)/\phi_{plateau}$ vs $x/R_{g0}$) for different chain lengths and slit widths and the agreement with the theoretically predicted exponent.[31,32] In athermal solutions, $\gamma$ is 0.13−0.20 at low concentrations in a broad slit to have $\phi(x)/\phi_{plateau} \sim ((x + \gamma)/R_{g0})^{1.69}$, the theoretically predicted power law. For Θ chains (PP model), $\gamma \cong 0.30$ was more appropriate than any other value.[33] Polymer segments sense the wall at a distance of $\gamma$ behind the physical wall.[31] Even with adding $\gamma$ to $x$, the two sets of SP data are still not on a common line, and each profile is on a power law with an exponent of ca. $^4/_3$ at $(x + \gamma)/R_{g0} < 0.8$. The upward deviation at $(x + \gamma)/R_{g0} < 0.2$ remains.

Next we examine the segment density profiles in a narrower slit at different $\phi_{av}$ obtained by using the two models for the Θ condition. Three pairs of profiles in
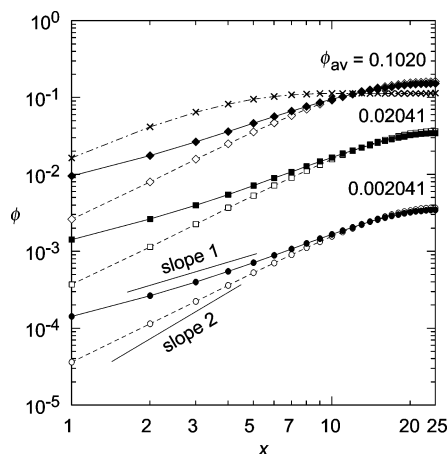
**Figure 11.** Segment density profile of $\Theta$ chains ($N = 1000$) in a slit of $D = 50$, plotted as a function of the distance from the wall, $x$. Results obtained in the SP model (closed symbols, solid lines) and the PP model (open symbols, dashed lines) are compared for three pairs of the average volume fraction, $\phi_{av}$ = 0.002041, 0.02041, and 0.1020. For $\phi_{av} = 0.1020$, the profile obtained for athermal chains is also shown (crosses).
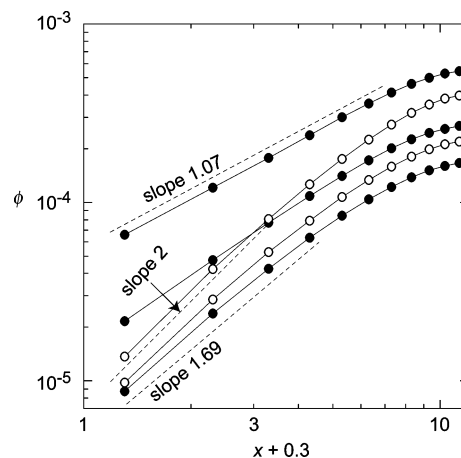


**Figure 12.** Segment density profile of polymer chains of $N = 500$ in the SP and PP models of various values of $\chi$ in the slit of $D = 24$, plotted as a function of the distance $x$ from the wall plus penetration depth $\gamma = 0.3$. The close circles represent the results for the SP model with $\chi/Z = 0$, 0.075, and 0.13465 from bottom to top. The open circles are for the PP model with $\chi/Z$ = 0.075 and 0.13465.
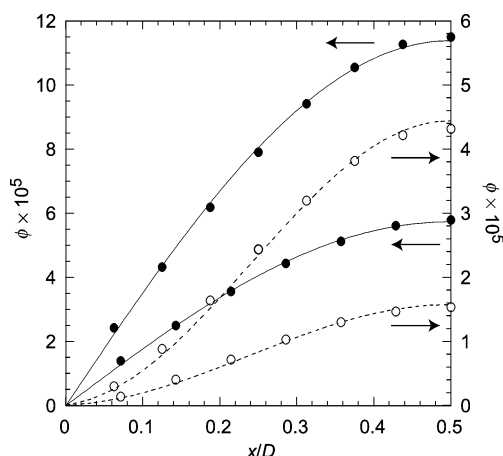
Figure 11 were obtained for chains of $N = 1000$ in a slit of $D = 50$ at $\phi_{av} = 0.002041$, 0.02041, and 0.1020. For reference, the profile of athermal chains at $\phi_{av} = 0.1020$ is shown also. The three profiles at $\phi_{av} = 0.1020$ are identical to those in Figure 3. Note that $2R_{g0}/D \cong 0.70$ in the $\Theta$ condition. The profiles do not have a plateau except the athermal chains at $\phi_{av} = 0.1020$. The profiles at $\phi_{av} = 0.002041$ can be overlaid onto the corresponding profiles at $\phi_{av} = 0.02041$ by translating vertically, indicating that at the latter concentration the three-body interaction between polymer segments (directly or through absence of intervening solvent molecules) is still too weak to change the profiles. As in a weak confinement (Figure 10), $\phi(x)$ at $x \leq 7$ is on a straight line with a slope less than two for the PP model. Adding $\gamma = 0.30$ to $x$ brings the slope to the theoretically predicted value. In contrast, $\phi(x)$ of the SP model shows a deviation from a power law even with added $\gamma$.

The way $\phi(x)$ decreases on approaching the wall is different between the athermal chains and $\Theta$ chains. Then, the profiles obtained in simulations under intermediate solvent conditions should exhibit a transition between the two behaviors of $\phi(x)$. Figure 12 shows profiles obtained in some of the simulations described for Figure 7. The concentration is sufficiently low. The width of $D = 24$ gives intermediate confinement strength. The value of $2R_{g0}/D$ is 1.02 for $\Theta$ chains and 1.40 for athermal chains. To exemplify the effectiveness of the penetration depth, $\gamma = 0.3$ is being added to $x$. In the series of data within the PP model, the exponent increases from 1.69 to 2 with decreasing $\epsilon_{pp}$ from 0 to $-0.2693$. The added $\gamma$ is too large for the athermal chains, and therefore there is a downward deviation in the first layer. In the SP models, in contrast, the exponent decreases from 1.69 to 1.07 with increasing $2\epsilon_{sp}$ from 0 to 0.2693.

Figure 13 compares $\phi(x)$ of $\Theta$ chains ($N = 500$) in the SP model and the PP model in strong confinement. Two values of $2R_{g0}/D$, 1.53 and 1.75, were used for each of the two models. The profiles of the PP chains can be fit with $\sim\sin^2(\pi x/D)$ which is shown as dashed lines. The good fitting is also a testimony to the nearly ideal nature of $\Theta$ chains.[33] The fitting improves when $\gamma = 0.3$ is added to $x$ and $2\gamma$ to $D$. The good fitting indicates



**Figure 13.** Segment density profiles of strongly confined $\Theta$ chains ($N = 500$) in slits of $D = 14$ and 16 at low concentrations, plotted as a function of the position in the slit, $x/D$. (a) SP model (closed circles); (b) PP model (open circles). The lines are fitting curves.

dominance of the ground-state mode: In the Fourier decomposition of the $x$-component of the Green function, $G(x,x';N)$, for a Gaussian chain confined by neutral walls ($\chi_{pw} = 0$), the ground state is given as $\sim\sin(\pi x/D)$ sin-$(\pi x'/D)$, and the corresponding segment density is $\sim\sin^2(\pi x/D)$.[40]

The profiles of the SP model are different. They are rather well fit by $\sim\sin(\pi x/D)$. Adding $\gamma$ does not make it any better. Since we are not aware of any theories that give an analytical expression of $\phi(x)$ for the chains confined by a pair of walls with $\chi_{pw} \neq 0$ (weakly interacting walls), we do not discuss the profiles of the SP chains further.

The inset of Figure 6 shows $\phi_1/\phi_{av}$ as a function of $D$ for three chain lengths of the SP model. Except for small $D$, all of the data are on a common straight line with a slope of $-1$. Simple geometrical consideration gives $\phi_1/\phi_{av} \sim D^{-1}$ for the density profile of the SP model under strong confinement, in agreement with the results in the inset.

The negative $\chi_{pw}$ in the SP model increases the segment density at sites near the walls compared with the PP model. Consequently, the SP chain receives a
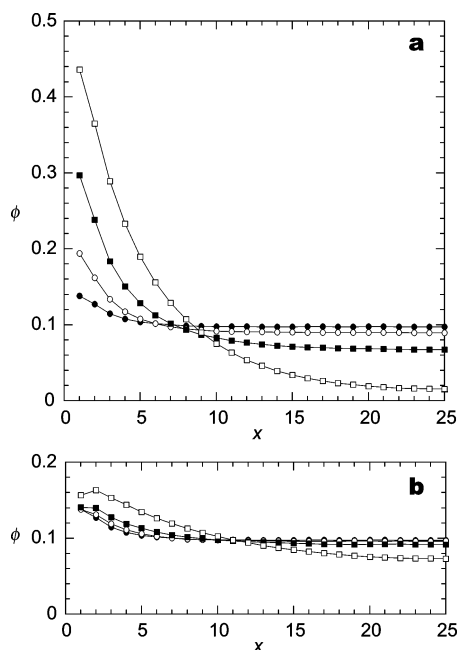
**Figure 14.** Segment density profiles of Θ chains ($N = 1000$, $D = 50$) in the presence of weak attraction, $\epsilon_{pw}/k_B T = -0.3$, between the wall and a polymer segment. (a) SP model with solvent qualities $2\epsilon_{sp}/k_B T = 0$ (closed circles), 0.1 (open circles), 0.2 (closed squares), and 0.2693 (open squares); (b) PP model with $\epsilon_{pp}/k_B T = 0$ (closed circles), $-0.1$ (open circles), $-0.2$ (closed squares), and $-0.2693$ (open squares).

greater entropy reduction. Note that the density profiles of the PP chains that are free from interactions with the walls is a result of minimization of the free energy, which is mostly entropic. The negative $\chi_{pw}$ in the SP model deviates $\phi(x)$ from the entropy maximum, but of course $\phi(x)$ is a result of the free energy minimization. Now we understand why the data for the SP model are above those for the PP model in Figure 6 and in the inset of Figure 7.

A difference between the two models can be observed when negative interaction $\epsilon_{pw}$ between polymer segments and the wall is explicitly introduced. Considering this situation is important in understanding experimental results obtained in various chromatographic methods.[17] Figure 14 compares the segment density profiles for chains of $N = 1000$ in a slit of $D = 50$ obtained in the two models under $\epsilon_{pw}/k_B T = -0.3$ and $\phi_{av} = 0.1020$. Part a is for the SP chains with different values of $\epsilon_{sp}$, and part b is for the PP chains with the values of $\epsilon_{pp}$ that give the values of $\chi$ identical to those in part a.

Part a exhibits a large difference between the profiles. There is a strong surface enrichment in the SP model. When the wall is slightly adsorptive ($\epsilon_{pw}/k_B T = -0.3$), a small change in the solvent quality causes a large difference in the profile. In contrast, the PP model is close to a compensation point where the surface depletion by conformational entropy loss and the surface enrichment by attractive walls are balanced to exhibit a flat density profile at the walls. From athermal to Θ solvents, the profile changes only slightly. This figure illustrates how the SP model accounts for adsorption in a poorer solvent whereas the PP model fails because of neglect of missing SP contacts for chains at the wall.

For a given $N$, $D$, and $\phi_{av}$, the profile is determined by $\chi$ and $\chi_{pw}$. The SP model with $\epsilon_{pw}/k_B T = -0.3$ and $2\epsilon_{sp}/k_B T = 0.2693$, for instance, should behave identi-

cally to the PP model with $\epsilon_{pw}/k_B T = -0.43465$ and $\epsilon_{pp}/k_B T = -0.2693$.

With a further decrease in $\epsilon_{pw}$, the profiles become more strongly governed by the adsorption (not shown). The difference between the profiles of the two models becomes smaller. When $\phi(x)$ climbs at the wall, the density in the middle of the slit is depleted. Then, an increase in the wall distance results in nearly zero density at the center at low concentration. It means that a part of any chain is always in contact with the walls.

## 5. Conclusions

We have shown that using the original PP model in a solvent condition other than athermal solvent to study the effect of confinement or of the walls introduces artificial repulsive interactions between the polymer and the walls. In contrast, the SP model, governed by polymer segment−solvent interactions, naturally introduces effective attraction between the walls and polymer segments when the solvent is near Θ, in agreement with experimental observations. The SP model allows more chains into the slit in equilibrium with the surrounding solution and increases the segment density near the walls. The difference between the two models is most obvious in the Θ condition when the walls exert slightly attractive interaction on polymer chains.

An SP model can be implemented in off-lattice systems as well. A study addressing the difference between an SP model and a PP model in off-lattice Monte Carlo simulations is being planned.

## References and Notes

(1) Frenkel, D.; Smit, B. *Understanding Molecular Simulation: From Algorithms to Applications*; Academic Press: San Diego, 1996.
(2) McCrackin, F. L.; Mazur, J.; Guttman, C. M. *Macromolecules* **1973**, *6*, 859.
(3) Olaj, O. F.; Pelinka, K. H. *Makromol. Chem.* **1976**, *177*, 3413.
(4) Meirovitch, H.; Lim, H. A. *J. Chem. Phys.* **1990**, *92*, 5144.
(5) Grassberger, P.; Hegger, R. *J. Chem. Phys.* **1995**, *102*, 6881.
(6) Milchev, A.; Binder, K. *Macromol. Theory Simul.* **1994**, *3*, 915.
(7) Rubio, A. M.; Freire, J. J.; Clarke, J. H. R.; Yong, C. W.; Bishop, M. *J. Chem. Phys.* **1995**, *102*, 2277.
(8) Ingersent, K.; Klein, J.; Pincus, P. *Macromolecules* **1990**, *23*, 548.
(9) Cherayil, B. J.; Kholodenko, A. L.; Freed, K. F. *J. Chem. Phys.* **1987**, *86*, 7204.
(10) Janssen, R. H. C.; Wang, S.; Nies, E.; Cifra, P. *Macromolecules* **1999**, *32*, 471.
(11) Buta, D.; Freed, K. F. Szleifer, I. *J. Chem. Phys.* **2000**, *112*, 6040.
(12) Milchev, A.; Binder, K. *Macromolecules* **1996**, *29*, 343.
(13) Cifra, P.; Bleha, T.; Wang, Y.; Teraoka, I. *J. Chem. Phys.* **2000**, *113*, 8313.
(14) Cifra, P.; Bleha, T. *Macromolecules* **2001**, *34*, 605.
(15) Teraoka, I.; Cifra, P. *J. Chem. Phys.* **2001**, *115*, 11362.
(16) Metzger, S.; Müller, M.; Binder, K.; Baschnagel, J. *Macromol. Theory Simul.* **2002**, *11*, 985.
(17) Berek, D. *Prog. Polym. Sci.* **2000**, *25*, 873.
(18) Panagiotopoulos, A. Z.; Wong, V.; Floriano, M. A. *Macromolecules* **1998**, *31*, 912.
(19) Meirowitch, L. *J. Chem. Phys.* **1988**, *88*, 4498, 4507.
(20) Grassberger, P.; Hegger, R. *Phys. Rev. E* **1995**, *51*, 2674.

(21) Hegger, R.; Grassberger, P. *J. Phys. A* **1994**, *27*, 4069.
(22) Jiang, J.; Liu, H.; Hu, Y. *Macromol. Theory Simul.* **1998**, *7*, 105.
(23) Jimenez, J.; de Joannis, J.; Bitsanis, I.; Rajagopalan, R. *Macromolecules* **2000**, *33*, 7157.
(24) Škrinárová, Z.; Bleha, T.; Cifra, P. *Macromolecules* **2002**, *35*, 8896.
(25) Cifra, P. *Macromol. Theory Simul.* **2003**, *12*, 270.
(26) Yethiraj, A.; Hall, C. K. *Mol. Phys.* **1991**, *73*, 503.
(27) Wang, Y.; Teraoka, I. *Macromolecules* **1997**, *30*, 8473.
(28) Plueddemann, E. P. *Silane Coupling Agents*, 2nd ed.; Plenum: New York, 1991.
(29) Metropolis, N.; Rosenbluth, A. W.; Rosenbluth, M. N.; Teller, A. H.; Teller, E. *J. Chem. Phys.* **1953**, *21*, 1087.
(30) Wang, Y.; Teraoka, I. *Macromolecules* **2000**, *33*, 3478.
(31) de Gennes, P. G. *Macromolecules* **1981**, *14*, 1637.
(32) Eisenriegler, E. *Phys. Rev. E* **1997**, *55*, 3116.
(33) Teraoka, I.; Cifra, P.; Wang, Y. *Macromolecules* **2001**, *34*, 7121.
(34) Teraoka, I.; Cifra, P.; Wang, Y. *Colloids Surf. A.* **2002**, *305*, 206.
(35) Teraoka, I. *Polymer Solutions: An Introduction to Physical Properties*; John Wiley: New York, 2002.
(36) Raphael, E.; Pincus, P. *J. Phys. II* **1992**, *2*, 1341.
(37) van Vliet, J. H.; Luyten, M. C.; ten Brinke, G. *Macromolecules* **1992**, *25*, 3802.
(38) Milchev, A.; Binder, K. *Eur. Phys. J. B* **1998**, *3*, 477; **2000**, *13*, 607.
(39) De Joannis, J.; Jimenez, J.; Rajagopalan, R.; Bitsanis, I. *Europhys. Lett.* **2000**, *51*, 41.
(40) de Gennes, P. G. *Scaling Concept in Polymer Physics*; Cornell University Press: Ithaca, NY, 1979.